

## ANALYSIS OF REFLECTION GRATINGS BY MEANS OF A MATRIX METHOD APPROACH

**J. Francés<sup>1,\*</sup>, C. Neipp<sup>1,2</sup>, A. Márquez<sup>1,2</sup>, A. Beléndez<sup>1,2</sup>, and I. Pascual<sup>2,3</sup>**

<sup>1</sup>Department of Physics, Systems Engineering and Signal Theory, Universidad de Alicante, Alicante E-03080, Spain

<sup>2</sup>University Institute of Physics to Sciences and Technologies, University of Alicante, Alicante E-03080, Spain

<sup>3</sup>Department of Optics, Pharmacology and Anatomy, University of Alicante, Alicante E-03080, Spain

**Abstract**—In this work, a matrix method is applied to study the propagation of electromagnetic waves inside a non-slanted reflection grating. The elements of the matrix which characterizes the periodic medium are obtained in terms of Mathieu functions and their derivatives, and the expressions of the efficiencies of reflected and transmitted orders are calculated in terms of the elements of the matrix. In addition the band structure of a general reflection grating is studied with the layer matrix of one single period. The results obtained by this matrix method are firstly compared to the results obtained by Kogelnik's expressions in index-matched media showing good agreement. The comparison is also made for a reflection grating embedded in two media with different refractive indexes, showing good agreement with an FDTD method, but slight differences with respect to Kogelnik's Coupled Wave Theory.

### 1. INTRODUCTION

The theory of propagation of electromagnetic waves in periodic media is well-developed [31]. One of the most predictive and popular theories to calculate the efficiency of the orders that propagate inside a diffraction grating [32, 33] is the Kogelnik's Coupled Wave

---

*Received 4 May 2011, Accepted 9 June 2011, Scheduled 30 June 2011*  
\* Corresponding author: Jorge Frances (jfmonllor@ua.es).

Theory [1, 34, 35]. The analytical expressions obtained with Kogelnik's Theory predict the response of the efficiency of the zeros and first order for volume phase gratings, for both reflection and transmission gratings. Nonetheless, since this theory disregard the second derivatives in the coupled wave equations derived from Maxwell equations, it does not account for boundary conditions. Moreover only two orders are supposed, so when either the thickness is low or when high refractive index modulations are recorded in the element Kogelnik's Theory deviates from the expected results. In these cases, the Coupled Wave theory (CW) allowing for more than two orders or the Rigorous Coupled Wave theory (RCW) [2] which does not disregard second derivatives in the coupled wave equations as does CW, are needed. The Rigorous Coupled Wave theory has been applied with success to volume holograms and binary gratings [3–9], photonic band structures [10], diffractive lenses [11], optical waveguides [12], anisotropic media [13], etc. Although exact predictions can be obtained by using RCW method it is still interesting to work with other more simple (also accurate) methods in specific cases. One of the most important situation in which the RCW analysis is not valid is for non-slanted reflection gratings. In this case, the modulation is no longer infinitely periodic since it has only a finite number of cycles. That causes the grating not to be strictly periodic and the Floquet Theorem, which is the basis for the modal and the coupled-wave analysis, can not be applied. For that reason, usually the slanted angle has been considered small, and as it approaches zero, all the reflected wave vectors in the incident medium approach a common direction, and the resulting reflected intensity of the composite wave is  $\sum_i |R_i|^2$ . The transmitted wave vectors and intensity follows the same behavior.

Recently a matrix-method approach has been used to evaluate the electromagnetic wave transmission for a one-dimensional reflection grating (normal incidence) [14]. Matrix methods have been successfully used to study the propagation of electromagnetic radiation in generally stratified media. Basically, the idea is to define a matrix which characterize the medium, linking the electromagnetic field components at an interface between two adjoining layers. By matrix multiplication the matrix of a complex medium (divided in regions with different laws of the dielectric permittivity) can be obtained. In this paper, we apply a matrix method to study the propagation of electromagnetic waves in non-slanted reflection gratings for an arbitrary angle of incidence. We will use the formalism introduced by Lekner [15], in which the matrix links the electric field and its derivative for any stratified medium, provided two particular solutions of Helmholtz equation are known.

## 2. THEORY

We will study the propagation of electromagnetic waves incident onto a non-slanted reflection grating whose relative dielectric permittivity varies in the form:

$$\epsilon(z) = \epsilon_{r0} + \epsilon_{r1} \cos(Kz), \quad (1)$$

where  $\epsilon_{r0}$  and  $\epsilon_{r1}$  are the average and the modulation of the dielectric permittivity respectively.  $K$  is the grating vector modulus related to the grating period,  $\Lambda$ , in the following way:

$$K = 2\pi/\Lambda. \quad (2)$$

The geometry is specified in Figure 1, where we will assume that the reflection grating is embedded in two media of indexes  $n_I$  and  $n_{II}$ .

For TE polarization the electric fields in media I and II are described as:

$$E^I = [\exp(ik_z^I z) + R \exp(-k_z^I z)] \exp(i(k_x x - \omega t)), \quad (3)$$

$$E^{II} = T \exp(ik_z^{II} z) \exp(i(k_x x - \omega t)), \quad (4)$$

where  $\omega$  is the angular frequency,  $k_x$  is the  $x$  component of the wave vectors;

$$k_x = n_I k_0 \sin \theta_I = n_{II} k_0 \sin \theta_{II}, \quad (5)$$

being  $k_0 = 2\pi/\lambda_0$ ,  $\lambda_0$  the wavelength in vacuum,  $\theta_I$  and  $\theta_{II}$  the angles between the wave vector and the normals to the corresponding homogeneous substrates. Therefore, the component of the wave vector in  $z$  direction in mediums I and II can be defined as follows:

$$k_z^I = n_I k_0 \cos \theta_I, \quad (6)$$

$$k_z^{II} = n_{II} k_0 \cos \theta_{II}, \quad (7)$$

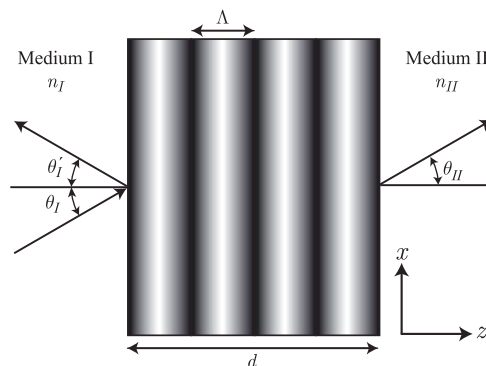


**Figure 1.** Illustration of the geometry of a diffraction grating.

whereas inside the periodic medium, the electric field is described as:

$$E = E(z) \exp[i(k_x x - \omega t)]. \quad (8)$$

## 2.1. Matrix Formalism

Inside the periodic medium,  $E(z)$  verifies the following second order differential equation:

$$\frac{d^2 E}{dz^2} + (k_0^2 \epsilon(z) - k_x^2) E = 0. \quad (9)$$

Let  $E_{c_1}$ ,  $E_{c_2}$  be two linearly independent solutions of Eq. (9). Lets also suppose that the medium extends from  $z = z_1$  to  $z = z_2$ . Following Lekner's discussion [15] a layer matrix  $\mathbf{M}$  can be built linking the fields and their derivatives at two different values of  $z$  in the following way:

$$\begin{pmatrix} E(z_2) \\ \frac{d}{dz} E(z_2) \end{pmatrix} = \mathbf{M} \begin{pmatrix} E(z_1) \\ \frac{d}{dz} E(z_1) \end{pmatrix}, \quad (10)$$

or

$$\begin{pmatrix} E(z_2) \\ \frac{d}{dz} E(z_2) \end{pmatrix} = \begin{pmatrix} m_{11} & m_{12} \\ m_{21} & m_{22} \end{pmatrix} \begin{pmatrix} E(z_1) \\ \frac{d}{dz} E(z_1) \end{pmatrix}, \quad (11)$$

where  $\mathbf{M}$  has the form:

$$\mathbf{M} = W^{-1} \begin{pmatrix} -\left(\frac{d}{dz} E_{c_1}, E_{c_2}\right) & (E_{c_1}, E_{c_2}) \\ -\left(\frac{d}{dz} E_{c_1}, \frac{d}{dz} E_{c_2}\right) & (E_{c_1}, \frac{d}{dz} E_{c_2}) \end{pmatrix}, \quad (12)$$

$$W = E_{c_1} \frac{d}{dz} E_{c_2} - E_{c_2} \frac{d}{dz} E_{c_1}. \quad (13)$$

$W$  is the Wronskian of the two independent solutions, which is constant, being the layer matrix  $\mathbf{M}$  unimodular, and:

$$(E_{c_1}, E_{c_2}) = E_{c_1}(z_1) E_{c_2}(z_2) - E_{c_2}(z_1) E_{c_1}(z_2), \quad (14)$$

$$\left(\frac{d}{dz} E_{c_1}, E_{c_2}\right) = E_{c_2}(z_2) \frac{d}{dz} E_{c_1}(z_1) - E_{c_1}(z_2) \frac{d}{dz} E_{c_2}(z_1), \quad (15)$$

$$\left(E_{c_1}, \frac{d}{dz} E_{c_2}\right) = E_{c_1}(z_1) \frac{d}{dz} E_{c_2}(z_2) - E_{c_2}(z_1) \frac{d}{dz} E_{c_1}(z_2), \quad (16)$$

$$\left(\frac{d}{dz} E_{c_1}, \frac{d}{dz} E_{c_2}\right) = \frac{d}{dz} E_{c_1}(z_1) \frac{d}{dz} E_{c_2}(z_2) - \frac{d}{dz} E_{c_2}(z_1) \frac{d}{dz} E_{c_1}(z_2). \quad (17)$$

Now, provided two independent solutions of Eq. (9) and taking into account Eqs. (13)–(17) and Eq. (12), the matrix  $\mathbf{M}$ , which characterizes a non-slanted reflection grating, can be built.

## 2.2. Solution in Terms of Mathieu Functions

In order to obtain the two linearly independent solutions of Eq. (9), one should notice that this equation can be transformed into the Mathieu equation:

$$\frac{d^2}{du^2} E + [a - 2q \cos(2u)] E = 0, \quad (18)$$

provided the following change of variables:

$$u = \frac{Kz}{2}, \quad (19)$$

$$a = \frac{4}{K^2} (k_0^2 \epsilon_{r0} - k_x^2), \quad (20)$$

$$q = -\frac{2}{K^2} k_0^2 \epsilon_{r1}. \quad (21)$$

Two linearly independent solutions of Eq. (18) are the Mathieu cosine  $C_m(a, q, u)$  and the Mathieu Sine  $S_m(a, q, u)$  verifying [16]:

$$\begin{aligned} C_m(a, q, 0) &= 1; & \frac{d}{dz} C_m(a, q, 0) &= 0, \\ S_m(a, q, 0) &= 0; & \frac{d}{dz} S_m(a, q, 0) &= 1. \end{aligned} \quad (22)$$

Any solution of Eq. (9) can therefore be put in the form:

$$E(z) = A C_m(a, q, Kz/2) + B S_m(a, q, Kz/2), \quad (23)$$

where  $A$  and  $B$  are arbitrary constants. So that the matrix  $\mathbf{M}$  of Eq. (9) can be built in terms of:

$$E_{c1} = C_m(a, q, Kz/2), \quad (24)$$

$$E_{c2} = S_m(a, q, Kz/2). \quad (25)$$

## 2.3. Boundary Conditions

For a reflection grating of thickness  $d$  the values of the reflectance and transmittance can be obtained by using Eqs. (11), (3) and (4), with  $z_1 = 0$  and  $z_2 = d$ .

$$\begin{pmatrix} T \exp(ik_z^H d) \\ ik_z^H T \exp(ik_z^H d) \end{pmatrix} = \mathbf{M} \begin{pmatrix} 1 + R \\ ik_z^I [1 - R] \end{pmatrix}. \quad (26)$$

So the reflection and transmission amplitudes can be obtained as:

$$R = \frac{k_z^I k_z^H m_{12} + m_{21} + ik_z^I m_{22} - ik_z^H m_{11}}{k_z^I k_z^H m_{12} - m_{21} + ik_z^I m_{22} - ik_z^H m_{11}}, \quad (27)$$

$$T = \exp(-ik_z^H d) \frac{2ik_z^I}{k_z^I k_z^H m_{12} - m_{21} + ik_z^I m_{22} - ik_z^H m_{11}} \quad (28)$$

Finally, the efficiency of the reflected order,  $DE_{-1}$ , can be obtained as:

$$DE_{-1} = |R|^2, \quad (29)$$

and the efficiency of the transmitted one:

$$DE_0 = \Re \left[ \frac{k_z^{II}}{k_z^I} \right] |T|^2, \quad (30)$$

## 2.4. Band Structure

In this section, it will be demonstrated how the study of one period of the grating provides sufficient information of the global structure.

Let  $\mathbf{M}$  be now the layer matrix of one period, which is constructed by using Eq. (12), in this case with  $z_1 = 0$  and  $z_2 = \Lambda$ . If a finite reflection grating consists of  $N$  periods, then the total matrix,  $\mathbf{M}_T$ , for the whole structure is obtained by the  $N$ th power of  $\mathbf{M}$ . For an unimodular matrix [17] the following expression is verified:

$$\mathbf{M}_T = \begin{pmatrix} m_{11} & m_{12} \\ m_{21} & m_{22} \end{pmatrix}^N = \begin{pmatrix} m_{11}S_N - S_{N-1} & m_{12}S_N \\ m_{21}S_N & m_{22}S_N - S_{N-1} \end{pmatrix}, \quad (31)$$

where

$$S_N = \frac{\sin(N\phi)}{\sin(\phi)}, \quad (32)$$

and

$$\cos \phi = \frac{1}{2} (m_{11} + m_{22}). \quad (33)$$

Therefore the efficiencies of the reflected and transmitted orders can be obtained by exactly the same analysis made in Section 2.3, but substituting matrix  $\mathbf{M}$  by matrix  $\mathbf{M}_T$  of Eq. (31). This gives an alternative approach to obtain the efficiencies of a non-slanted reflection grating.

The band structure of a non-slanted reflection grating can also be studied with the knowledge of the layer matrix of one period. As explained in [15], the Block factor  $\beta$  can be determined by the condition:

$$\det(\mathbf{M} - \beta \mathbf{I}) = 0. \quad (34)$$

Considering that  $\text{tr}\mathbf{M} = 2 \cos \phi$ , Eq. (33), and  $\det(\mathbf{M}) = 1$ :

$$\beta_{\pm} = \cos \phi \pm (\cos^2 \phi - 1)^{1/2}. \quad (35)$$

The band edges are given by  $\cos^2 \phi = 1$ , whereas  $\cos^2 \phi > 1$  gives the band gaps of the grating. Therefore, the condition  $\text{tr}\mathbf{M} = \pm 2$  gives us the band edges.

For our particular case:

$$\text{tr}\mathbf{M} = \frac{1}{W} \left[ - \left( \frac{dE_{c1}}{dz}, E_{c2} \right) + \left( E_{c1}, \frac{dE_{c2}}{dz} \right) \right], \quad (36)$$

with  $E_{c1}$  and  $E_{c2}$  given by Eq. (24) and Eq. (25).

Lets assume a low dielectric constant modulation ( $\epsilon_{r1} \sim 0$ ), in Eq. (21) that implies  $q \sim 0$ . In this case [18]:

$$E_{c1} = C_m(a, 0, Kz/2) \approx \cos(\sqrt{a}Kz/2), \quad (37)$$

$$E_{c2} = S_m(a, 0, Kz/2) \approx \sin(\sqrt{a}Kz/2). \quad (38)$$

Evaluating  $\text{tr}\mathbf{M}$  in the interval  $[0, \Lambda]$ , we have:

$$\left( \frac{dE_{c1}}{dz}, E_{c2} \right) = -\frac{\sqrt{a}K}{2} \cos(\sqrt{a}K\Lambda/2), \quad (39)$$

$$\left( E_{c1}, \frac{dE_{c2}}{dz} \right) = \frac{\sqrt{a}K}{2} \cos(\sqrt{a}K\Lambda/2), \quad (40)$$

$$W(0) = W(\Lambda) = \frac{\sqrt{a}K}{2}. \quad (41)$$

Therefore Eq. (36) takes the form:

$$\text{tr}\mathbf{M} = 2 \cos(\sqrt{a}\pi). \quad (42)$$

From Eq. (42), one can see that  $|\text{tr}\mathbf{M}| \leq 2$ , so no stop bands exist, but strong reflection occur at the band edges characterized by the condition  $\text{tr}\mathbf{M} = \pm 2$ , which using Eq. (42) leads to the following condition:

$$\cos(\sqrt{a}\pi) = \pm 1 \rightarrow \sqrt{a} = 1, \quad (43)$$

thus, from Eq. (20):

$$\frac{2}{K} \sqrt{k_0^2 \epsilon_{r0} - k_x^2} = 1, \quad (44)$$

or

$$\frac{2\pi}{\lambda} n_0 \cos \theta_B = \frac{\pi}{\Lambda} \rightarrow \cos \theta_B = \frac{\lambda}{2n_0 \Lambda}, \quad (45)$$

where  $\theta_B$  is the angle of the incident wave inside the periodic medium and  $n_0 = \sqrt{\epsilon_{r0}}$ .

The Eq. (45) is just Bragg Condition for non-slanted reflection gratings. Although in order to obtain Eq. (45) no refractive index modulation has been assumed, it must be taken into account that Bragg condition is just a geometrical condition (without influence of  $\epsilon_{r1}$ ), so that Eq. (45) can be considered valid for every  $\epsilon_{r1}$ .

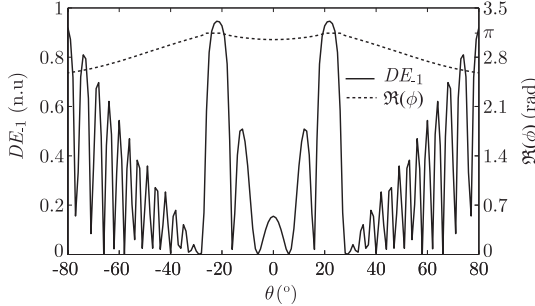


**Figure 2.** Real part of  $\phi$  and the reflectance as a function of the angle of incidence. The parameters of the grating where:  $\Lambda = 0.2 \mu\text{m}$ ,  $d = 15 \mu\text{m}$ ,  $\Delta n = 0.025$  and  $\lambda = 633 \text{ nm}$ .

In Figure 2, the real part of  $\phi$  (no imaginary part exists), is represented as a function of the angle of incidence for a reflection grating with period  $\Lambda = 0.2 \mu\text{m}$ , thickness  $d = 15 \mu\text{m}$  and refractive index modulation  $\Delta n = 0.025$ , the incident wavelength was chosen to be  $633 \text{ nm}$ . The reflectance as a function of the angle is also represented, where as expected strong reflection occurs at the band edges (Bragg angles).

## 2.5. Finite-difference Time-domain Method

The finite-difference time-domain method (FDTD) presents a robust and powerful approach to directly solve Maxwell's curl equation both in time and space. This technique is accurate solving complex elements over frequency domain methods [19, 20, 36–40], such as the method of moments (MoM). With FDTD method arbitrary shapes and inhomogeneous properties on the grid-space can be defined easily [41–46]. Moreover, this method is able to provide real-time pictures of the electromagnetic field. Concretely, the method solves in a self-consistent manner the Maxwell curl equations [21, 22]:

$$\frac{d\tilde{\mathbf{D}}}{dt} = \frac{1}{\sqrt{\epsilon_0 \mu_0}} (\nabla \times \mathbf{H} - \sigma \tilde{\mathbf{E}}), \quad (46)$$

$$\tilde{\mathbf{D}}(\omega) = \epsilon_r^*(\omega) \cdot \tilde{\mathbf{E}}, \quad (47)$$

$$\frac{d\mathbf{H}}{dt} = -\frac{1}{\sqrt{\epsilon_0 \mu_0}} \nabla \times \tilde{\mathbf{E}} - \frac{\sigma_m}{\mu_0} \mathbf{H}, \quad (48)$$

where  $\epsilon_0$  is the electrical permittivity in farads per meter,  $\epsilon_r^*$  is the medium's relative complex permittivity constant,  $\mu_0$  is the magnetic

permeability in henrys per meter,  $\sigma_m$  is an equivalent magnetic resistivity in ohms per meter and  $\sigma$  is the electric conductivity in siemens per meter. The flux density is denoted by  $\mathbf{D}$  and both  $\mathbf{D}$  and  $\mathbf{E}$  are normalized respect to the vacuum impedance  $\eta_0$ . The standard explicit central differencing scheme introduced by Yee [23] is applied. Although, the FDTD solution is straightforward for normal incidence case, a difficulty arises for the obliquely incident case. This is solved by means of a delay that cannot be solved directly using time-domain techniques (see, for instance, Refs. [21, 24]). One approach derives the differential equation that relates the displacement vector  $\mathbf{D}$  to the electric field  $\mathbf{E}$  and is solved simultaneously with Maxwell's equations at each time step. As shown in Figure 3, the simulation region is separated into a scattered-field region and a total-field region (incident plus scattered) where  $(\mathbf{E}, \mathbf{H})_{\text{total}} = (\mathbf{E}, \mathbf{H})_{\text{inc}} + (\mathbf{E}, \mathbf{H})_{\text{scat}}$ . The joining of these two regions is the source boundary.

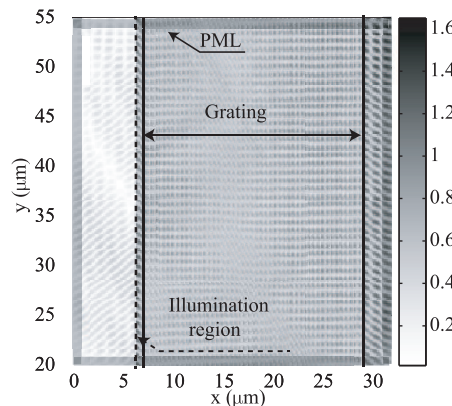


**Figure 3.** Time step picture of a diffraction grating simulation.

Another important feature in FDTD methods is a proper absorbing boundary condition to truncate the simulation region without artificial reflections. The perfectly matched layer absorbing boundary conditions proposed by Berenger [25], which have been found to be effective and to cause only slight reflection error, are used in our study. Although, in this work, a slight deviation from the Berenger method [26] will be made by introducing fictitious conductivities associated with  $\mathbf{D}$  and  $\mathbf{H}$ , instead of  $\mathbf{E}$  and  $\mathbf{H}$ . The basic idea of this formalism is to create a medium that is lossy and minimize the amount of reflection between free air and the PML region. The effect of this is to create a nonphysical absorbing medium adjacent to the outer FDTD mesh boundary that has a wave impedance independent of the angle

**Table 1.** Simulation parameters for the FDTD method applied to reflection holographic diffraction gratings.

$\lambda$	$\Delta$	$\Delta t$	$n_r$	$n_c$	$N_{\text{steps}}$	$N_{\text{PML}}$
632,1 nm	15.8 nm	$26.34 \cdot 10^{-9}$ ns	3072	1280	9000	12

of incidence and frequency of the outgoing scattered waves [29, 30]. There have been numerous approaches to this problem [24, 27, 28]. The basic problem-configuration dimensions are summarized in Figure 3, in which interaction of the electric field is shown. Each cell of simulation is a square of homogeneous material, and the values of this parameters inside the grating follows the sinusoidal variation of the refractive index, which is related with the dielectric permittivity as shown in Eq. (1).

### 3. RESULTS AND DISCUSSION

To validate the theoretical model previously developed will now conduct a comparison between the results obtained using the proposed matrix method (MM) with the ones obtained by using the coupled wave theory of Kogelnik (TK). The simulations are performed for a reflection grating with a period of  $0.2 \mu\text{m}$ , an average index  $n_0 = 1.63$  and a modulation index of 0.025, for a wavelength of 633 nm. Figure 4(a) shows the diffraction efficiency of order  $-1$  as a function of the angle of incidence for a grating of thickness  $d = 10 \mu\text{m}$ . As shown in the figure the degree of agreement between the two theories is quite good indicating the validity of the model.

On the other hand in Figure 4(b) is represented the diffraction efficiency for order  $-1$  as a function of the angle of incidence for a grating of thickness  $d = 20 \mu\text{m}$ , again a great similarity between the results can be seen, although some discrepancies appear far from the Bragg angle. These discrepancies are due to the fact that Kogelnik's theory makes some assumptions, whether the one proposed not. In Figure 4(c) the diffraction efficiency of order  $-1$  as a function of the angle is shown for a grating of  $d = 10 \mu\text{m}$ , but in this case the grating presents a higher index modulation,  $\Delta n = 0.055$ . It is clearly observed, that although the two theories lead to almost the same results, now there are more discrepancies between them than in previous cases. This is due to the fact that when the modulation index is high, the Kogelnik theory begins to lose validity. Finally, Figure 5 shows the diffraction efficiency of order  $-1$  as a function of the wavelength for a grating of thickness  $d = 10 \mu\text{m}$  and a modulation index of 0.025, for normal incidence, proving once again good agreement between both theories.

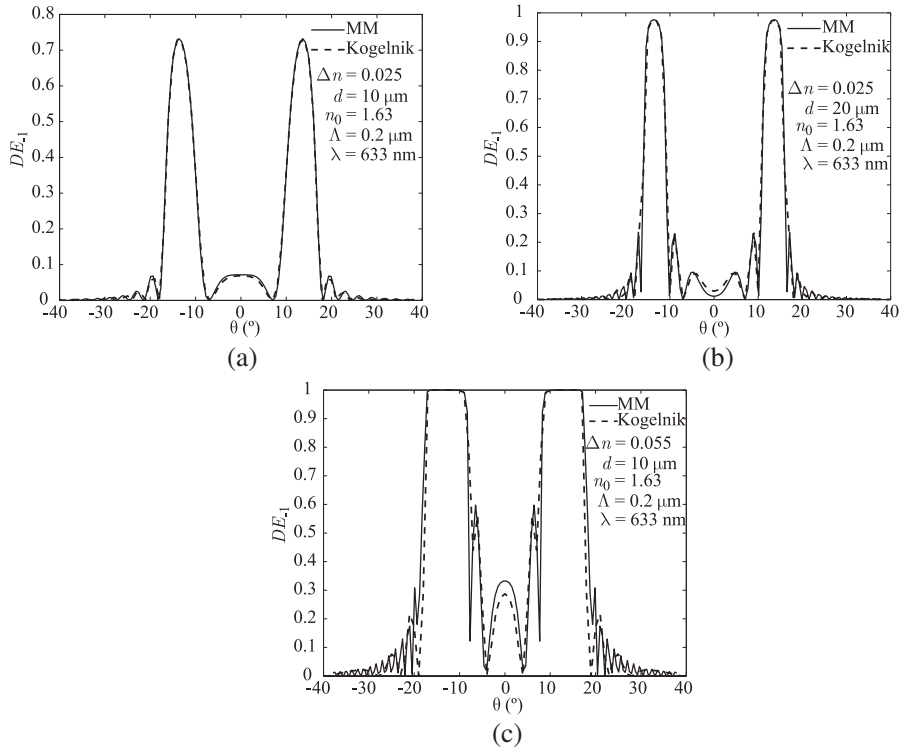


**Figure 4.** Diffraction efficiency as a function of the angle of incidence with the following parameters: (a)  $\Lambda = 0.2 \mu\text{m}$ ,  $d = 10 \mu\text{m}$ ,  $n_0 = 1.63$ ,  $\Delta n = 0.025$ ,  $\lambda = 633 \text{ nm}$ . (a)  $\Lambda = 0.2 \mu\text{m}$ ,  $d = 20 \mu\text{m}$ ,  $n_0 = 1.63$ ,  $\Delta n = 0.025$ ,  $\lambda = 633 \text{ nm}$ . (c)  $\Lambda = 0.2 \mu\text{m}$ ,  $d = 10 \mu\text{m}$ ,  $n_0 = 1.63$ ,  $\Delta n = 0.055$ ,  $\lambda = 633 \text{ nm}$ .

Although there is a good agreement between the proposed matrix method and the coupled wave theory of Kogelnik (TK) under several conditions, differences between the two methods becomes greater when the two media beside the input and output plane of the grating present different refractive indexes than that of the grating substrate. These differences are shown in Figure 6, where the diffraction efficiency for order  $-1$  obtained via MM, TK and FDTD as a function of the angle of incidence are represented. The simulation parameters related with the FDTD method are detailed in Table 1, where  $\Delta$  and  $\Delta t$  are the spatial and time resolutions respectively. The relationship between  $\Delta$  and  $\Delta t$  ensures numerical stability and convergence [24]. The FDTD grid is based on an matrix for each field component with  $n_r \times n_c$

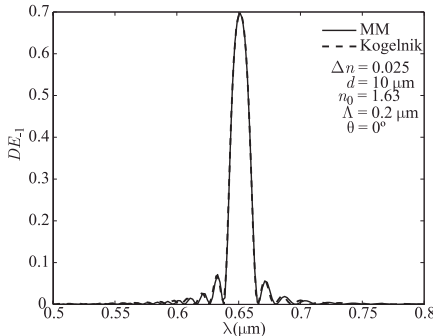


**Figure 5.** Diffraction efficiency as a function of the wavelength for grating with the following parameters:  $\Lambda = 0.2 \mu\text{m}$ ,  $d = 10 \mu\text{m}$ ,  $n_0 = 1.63$ ,  $\Delta n = 0.025$ ,  $\theta = 0^\circ$ .

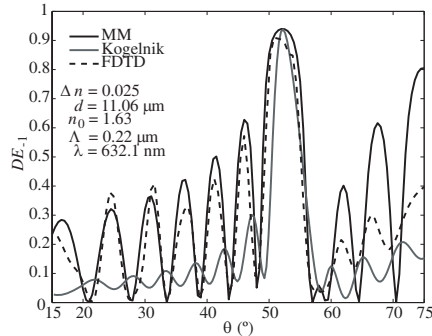


**Figure 6.** Diffraction efficiency as a function of the angle of incidence. Comparision between Mathieu's theory, Kogelnik's theory and also the FDTD method.

dimensions. The number of time steps ensures that the stationarity has been reached, and the number of PML cells has been fixed to 12 obtaining successful results. A good agreement between the numerical method and the MM method is achieved, but in this case coupled wave theory of Kogelnik response is different, mainly far from the Bragg angles. The discrepancies between MM and FDTD are produced basically by the fact that the FDTD method is based in a finite grid whereas analytical methods defines the input plane of the grating in an infinitely dimension. Nevertheless, as can be seen in Figure 6 results obtained with matrix and numerical method are quite similar compared with the pattern obtained via coupled wave theory of Kogelnik, the main differences appearing in the lateral lobes far from the Bragg angle.

#### 4. CONCLUSION

A matrix method has been developed to analyze the propagation of electromagnetic waves inside a non-slanted reflection grating. The elements of the layer matrix which characterizes the reflection grating are calculated in terms of Mathieu functions. In addition the band structure for a general non-slanted reflection grating is obtained by using the layer matrix corresponding to one single period demonstrating that no stop bands exist and that the band edges coincide with the Bragg angles of Kogelnik's Theory. This method is rigorous in the sense that no approximations are made, and the

results obtained by using this method have been compared to those obtained by Kogelnik's expressions, demonstrating good agreement when the reflection grating is embedded into media with the same index of refraction. Nonetheless slight differences exist when either the refractive index modulation is high or the reflection grating is embedded in two media with different refractive indexes.

In future work, it is also planned to evaluate the method in TM polarization. In this case the differential equation obtained must be solved by numerical techniques instead of the analytical expressions given by TE. Moreover, illuminating the grating with Gaussian beams should reduce the problems related with the finite dimensions of the plane wave currently used in the FDTD method.

## ACKNOWLEDGMENT

This work was supported by the "Ministerio de Ciencia e Innovación" of Spain under projects FIS2008-05856-C02-01 and FIS2008-05856-C02-02, and by the "Generalitat Valenciana" of Spain under project PROMETEO/2011/021.

## REFERENCES

1. Kogelnik, H., "Coupled wave theory for thick hologram gratings," *Bell Labs Tech. J.*, Vol. 48, No. 9, 2909–2947, 1969.
2. Moharam, M. G. and T. K. Gaylord, "Rigorous coupled-wave analysis of planar-grating diffraction," *J. Opt. Soc. Am.*, Vol. 71, No. 7, 811–818, 1981.
3. Moharam, M. G. and T. K. Gaylord, "Rigorous coupled-wave analysis of grating diffraction-e-mode polarization and losses," *J. Opt. Soc. Am.*, Vol 73 , No. 4, 451–455, 1983.
4. Moharam, M. G. and T. K. Gaylord, "Three-dimensional vector coupled-wave analysis of planar-grating diffraction," *J. Opt. Soc. Am.*, Vol. 73, No. 9, 1105–1112, 1983.
5. Moharam, M. G. and T. K. Gaylord, "Analysis and applications of optical diffraction by gratings," *Proc. IEEE*, Vol. 73, No. 5, 894–937, 1985.
6. Moharam, M. G. and T. K. Gaylord, "Rigorous coupled-wave analysis of metallic surface-relief gratings," *J. Opt. Soc. Am. A*, Vol. 3, No. 11, 1780–1787, 1986.
7. Moharam, M. G., E. B. Grann, D. A. Pommet, and T. K. Gaylord, "Formulation for stable and efficient implementation of the

rigorous coupled-wave analysis of binary gratings,” *J. Opt. Soc. Am. A*, Vol. 12, No. 5, 1068–1076, 1995.

- 8. Kamiya, N., “Rigorous coupled-wave analysis for practical planar dielectric gratings: 1. Thickness-changed holograms and some characteristics of diffraction efficiency,” *Appl. Optics*, Vol. 37, No. 25, 5843–5853, 1998.
- 9. Neipp, C., A. Beléndez, S. Gallego, M. Ortúñoz, I. Pascual, and J. Sheridan, “Angular responses of the first and second diffracted orders in transmission diffraction grating recorded on photopolymer material,” *Opt. Express*, Vol. 11, No. 16, 1835–1843, 2003.
- 10. Dansas, P. and N. Paraire, “Fast modeling of photonic bandgap structures by use of a diffraction-grating approach,” *J. Opt. Soc. Am. A*, Vol. 15, No. 6, 1586–1598, 1998.
- 11. Chang, N. Y. and C. J. Juo, “Algorithm based on rigorous coupled-wave analysis for diffractive optical element design,” *J. Opt. Soc. Am. A*, Vol. 18, No. 10, 2491–2501, 2001.
- 12. Little, B. E. and W. P. Huang, “Coupled-mode theory for optical waveguides,” *Progress In Electromagnetics Research*, Vol. 10, 217–270, 1995.
- 13. Jarem, J. M., “Rigorous coupled wave theory of anisotropic, azimuthally-inhomogeneous cylindrical systems,” *Progress In Electromagnetics Research*, Vol. 19, 109–127, 1998.
- 14. Carretero, L., M. Pérez-Molina, P. Acebal, S. Blaya, and A. Fimia, “Matrix method for the study of wave propagation in one-dimensional general media,” *Opt. Express*, Vol. 14, No. 23, 11385–11391, 2006.
- 15. Lekner, J., *Theory of Reflection of Electromagnetic and Particle Waves*, Kluwer Academic Publishers Group, 1987.
- 16. Abramowitz, M. and I. A. Stegun, *Handbook of Mathematical Functions*, Ch. 20, 722–748, Dover Publications, Inc., New York, 1972.
- 17. Abeles, F., *Optics of Thin Films in Advanced Optical Techniques*, North-Holland Publishing Co., Amsterdam, 1967.
- 18. Frenkel, D. and R. Portugal, “Algebraic methods to compute Mathieu functions,” *J. Phys. A: Math. Gen.*, Vol. 34, 3541–3351, 2001.
- 19. Vahabi Sani, N., A. Mohammadi, A. Abdipour, and F. M. Ghanouchi, “Analysis of multiport receivers using FDTD technique,” *Journal of Electromagnetic Waves and Applications*, Vol. 23, No. 5–6, 635–643, 2009.

20. Silva, A. O., R. Bertholdo, M. G. Chiavetto, B.-H. V. Borges, S. J. L. Ribeiro, Y. Messaddeq, and M. A. Romero, "Comparative analysis between experimental characterization results and numerical FDTD modeling of self-assembled photonic crystals," *Progress In Electromagnetics Research B*, Vol. 23, No. 19, 329–342, 2010.
21. Sullivan, D. M., *Electromagnetic Simulation Using the FDTD Method*, IEEE Press Editorial Board, 2000.
22. Balanis, C. A., *Advanced Engineering Electromagnetics*, Wiley, New York, 1989.
23. Yee, K. S., "Numerical solution of initial boundary value problems involving Maxwell's equations in isotropic media," *IEEE Trans. Antennas Propag.*, Vol. 14, No. 3, 302–307, 1996.
24. Taflove, A., *Computational Electrodynamics: The Finite-difference Time-domain Method*, Artech House Publishers, 1995.
25. Berenger, J. P., "A perfectly matched layer for the absorption of electromagnetic waves," *J. Comput. Phys.*, Vol. 114, No. 2, 185–200, 1994.
26. Sullivan, D. M., "A simplified PML for use with the FDTD method," *Microwave and Guided Wave Letters IEEE*, Vol. 6, No. 2, 97–99, 1996.
27. Kunz, K. S. and R. J. Luebbers, *The Finite Difference Time Domain Method for Electromagnetics*, CRC Press, 1993.
28. Pérez-Ocón, F., J. R. Jiménez, and A. M. Pozo, "Exponential discretization of the perfectly matched layer (PML) absorbing boundary condition simulation in FDTD 3D," *Optik*, Vol. 113, No. 8, 354–360, 2002.
29. Francés, J., C. Neipp, M. Pérez-Molina, and A. Beléndez, "Rigorous interference and diffraction analysis of diffractive optic elements using the finite-difference time-domain method," *Comput. Phys. Commun.*, Vol. 181, No. 12, 1963–1973, 2010.
30. Zheng, G., A. A. Kishk, A. W. Glisson, and A. B. Yakovlev, "Implementation of Mur's absorbing boundaries with periodic structures to speed up the design process using finite-difference time-domain method," *Progress In Electromagnetics Research*, Vol. 58, 101–114, 2006.
31. Zheng, G., B.-Z. Wang, H. Li, X.-F. Liu, and S. Ding, "Analysis of finite periodic dielectric gratings by the finite-difference frequency-domain method with the sub-entire-domain basis functions and wavelets," *Progress In Electromagnetics Research*, Vol. 99, 453–463, 2009.

32. Suyama, T., Y. Okuno, and T. Matsuda, "Surface plasmon resonance absorption in a multilayered thin-film grating," *Journal of Electromagnetic Waves and Applications*, Vol. 23, No. 13, 1773–1783, 2009.
33. Ni, J., B. Chen, S. L. Zheng, X.-M. Zhang, X.-F. Jin, and H. Chi, "Ultra-wideband bandpass filter with notched band based on electrooptic phase modulator and phase-shift fiber Bragg grating," *Journal of Electromagnetic Waves and Applications*, Vol. 24, No. 5–6, 795–802, 2010.
34. Liau, J.-J., N.-H. Sun, S.-C. Lin, R.-Y. Ro, J.-S. Chiang, C.-L. Pan, and H.-W. Chang, "A new look at numerical analysis of uniform fiber Bragg gratings using coupled mode theory," *Progress In Electromagnetics Research*, Vol. 93, 385–401, 2009.
35. Sun, N.-H., J.-J. Liau, Y.-W. Kiang, S.-C. Lin, R.-Y. Ro, J.-S. Chiang, and H.-W. Chang, "Numerical analysis of apodized fiber Bragg gratings using coupled mode theory," *Progress In Electromagnetics Research*, Vol. 99, 289–306, 2009.
36. Swillam, M. A., R. H. Gohary, M. H. Bakr, and X. Li, "Efficient approach for sensitivity analysis of lossy and leaky structures using FDTD," *Progress In Electromagnetics Research*, Vol. 94, 197–212, 2009.
37. Faghihi, F. and H. Heydari, "Time domain physical optics for the higher-order FDTD modeling in electromagnetic scattering from 3-D complex and combined multiple materials objects," *Progress In Electromagnetics Research*, Vol. 95, 87–102, 2009.
38. Zhang, Y.-Q. and D.-B. Ge, "A unified FDTD approach for electromagnetic analysis of dispersive objects," *Progress In Electromagnetics Research*, Vol. 96, 155–172, 2009.
39. Yang, S., Y. Chen, and Z.-P. Nie, "Simulation of time modulated linear antenna arrays using the FDTD method," *Progress In Electromagnetics Research*, Vol. 98, 175–190, 2009.
40. Xiao, S.-Q., Z. Shao, and B.-Z. Wang, "Application of the improved matrix type FDTD method for active antenna analysis," *Progress In Electromagnetics Research*, Vol. 100, 245–263, 2010.
41. Kalaei, P. and J. Rashed-Mohassel, "Investigation of dipole radiation pattern above a chiral media using 3D BI-FDTD approach," *Journal of Electromagnetic Waves and Applications*, Vol. 23, No. 1, 75–86, 2009.
42. Tay, W. C. and E. L. Tan, "Implementations of PMC and PEC boundary conditions for efficient fundamental ADI- and LOD-FDTD," *Journal of Electromagnetic Waves and Applications*, Vol. 24, No. 4, 565–573, 2010.

43. Dai, S.-Y., C. Zhang, and Z.-S. Wu, "Electromagnetic scattering of objects above ground using MRTD/FDTD hybrid method," *Journal of Electromagnetic Waves and Applications*, Vol. 23, No. 16, 2187–2196, 2009.
44. Li, J., L.-X. Guo, and H. Zeng, "FDTD method investigation on the polarimetric scattering from 2-D rough surface," *Progress In Electromagnetics Research*, Vol. 101, 173–188, 2010.
45. Xu, K., Z. Fan, D.-Z. Ding, and R.-S. Chen, "Gpu accelerated unconditionally stable crank-nicolson FDTD method for the analysis of three-dimensional microwave circuits," *Progress In Electromagnetics Research*, Vol. 102, 381–395, 2010.
46. Izadi, M., M. Z. A. Ab Kadir, C. Gomes, and W. F. W. Ahmad, "An analytical second-FDTD method for evaluation of electric and magnetic fields at intermediate distances from lightning channel," *Progress In Electromagnetics Research*, Vol. 110, 329–352, 2010.